Mitigating Point of Common Coupling Voltage Harmonics by Photovoltaic Inverter Using Extremum Seeking Control

S. M. Tababtabaei Jebeli[1], Seyed M. Madani[1*], M. Mojiri[2], E. Karimi[1]

[1] Faculty of Engineering, University of Isfahan, Hezar Jarib Ave., P.O. Box: 81746-73441, Isfahan, Iran

[2] Faculty of Electrical and Computer Engineering, Isfahan University of Technology, University Boulevard, Esteghlal Square, Isfahan, Iran

*Corresponding Author: m.madani@eng.ui.ac.ir

masoud.tabatabaei@eng.ui.ac.ir; mohsen.mojiri@cc.iut.ac.ir; karimi.ebrahim@gmail.com

Abstract— Growing nonlinear loads in modern grids cause higher harmonics, prompting new grid codes that require inverter-based sources to participate in harmonic mitigation. This paper presents a novel approach to mitigate harmonics in microgrids by utilizing the available capacity of Photovoltaic (PV) systems, merging clean energy production with enhanced power quality. The proposed control strategy employs Extremum Seeking Control (ESC) due to its maturity and ease of implementation. The ESC minimizes the Point of Common Coupling (PCC) voltage Total Harmonic Distortion (THD) when load and grid impedances are unknown. Controller parameter tuning depends on available inverter capacity and desired control performance. To mitigate PCC harmonic voltage, the PV injects a suitable harmonic current, in phase with the load harmonic current, ensuring maximum cancellation. The injected harmonic current magnitude remains lower than the load current magnitude, considering the available inverter capacity. Simulations in PSCAD validate this technique, demonstrating significant PCC voltage THD reduction without prior knowledge of the load current harmonic. Specifically, the voltage THD and the current THD with the ESC, are reduced to 0.29% and 2.40%. Performance comparisons with an Active Power Filter (APF) exhibit the ESC has superior performance (APF reduced voltage THD to 0.69% and current THD to 5.61%). These results demonstrate the ESC's effectiveness and potential as a viable solution for harmonic mitigation in microgrids, offering a significant improvement in power quality and supporting the increasing integration of renewable energy sources.

Keywords—Harmonics Mitigation, Power Quality, Extremum Seeking Control, Photovoltaic Systems, Microgrids.

Nomenclature

Abbreviation	Definition
AI	Artificial Intelligence
APF	Active Power Filter
CCM	Continuous Conduction Mode
DC	Direct Current
ESC	Extremum Seeking Control
FFT	Fast Fourier Transform
FRT	Fault Ride-Through
IEEE	Institute of Electrical and Electronics
MGs	Microgrids
MPC	Model Predictive Control
NSGA-II	Non-dominated Sorting Genetic Algorithm II
OF	Objective Function
PCC	Point of Common Coupling
PV	Photovoltaic
PWM	Pulse Width Modulation
SRF	Synchronous Reference Frame
THD	Total Harmonic Distortion
VCM	Voltage Control Method

1. Introduction

Solar energy offers an economical, proven renewable way to produce electricity, which restrains greenhouse gas emissions to meet energy goals. The Solar Energy Industry Association in 2021 increased its target to account for 30% of overall power production in the US by 2030 [1] while the preceding goal was 20%. According to the International Energy Agency Snapshot Reports 2023, the cumulative capacity of the global PV base experienced substantial growth in 2022, reaching approximately 1,185 GW, which occurred despite and in some cases due to the increase in prices following the COVID-19 pandemic and the geopolitical tensions in Europe. However, in situations where there is no sunlight or when the required power is supplied by the grid, this significant capacity can serve the purpose of mitigating harmonic currents, in the presence of nonlinear loads. This becomes particularly relevant in the current era, where nonlinear loads are prevalent.

The voltage and current of microgrids (MGs) are mainly polluted by nonlinear loads, switching devices, and resonance. Most MGs contain renewable resources that are connected to the network through power electronic devices. Due to the volatile nature of renewable resources, especially photovoltaics (PVs), they are not always functioning at their full capacity. Nonlinear operation of converters and PVs causes harmonic distortion. On the other hand, the available rating can be used to realize the ancillary services without additional costs [2]. Accordingly, the capacity of PVs can be used to superimpose the existing harmonic content of the grid [3]. The harmonic contents in most cases in MGs have a higher amount of Total Harmonic Distortion (THD) in the island mode than in the grid-connected mode. There are some instances during island operation, in which THD, as a measure of the level of distortion of a voltage caused by the presence of harmonics of nonlinear load, or even an individual harmonic, goes beyond the limits provided by the standards, namely IEEE 519-2014 or SS-EN 50160.

Traditionally, the harmonics in the distribution systems were mitigated by centralized active power filters or passive filters [4]. However, these techniques are single-purpose control strategies, which are inefficient, especially in today's economy-biased world [5]. Several pervasive reviews on the topic outlined different features of the issue. Table 1 provides a summary of key issues and techniques addressed in various references. Each row represents a specific topic or method related to power systems, such as voltage and frequency fluctuations, harmonics distortion, fault ride-through (FRT) capability, reactive power support, mitigation techniques, and control algorithms. The columns correspond to individual references, with an "×" indicating that the particular topic or technique is covered in that reference. This table serves as a concise comparative analysis, highlighting the focus areas of each reference and offering an overview of the breadth and depth of the surveyed literature.

A method for mitigating harmonics has been proposed in [16] which watches out for the load dynamics. A decoupled control of active and reactive power by capacitive virtual impedance was implemented to improve harmonic current sharing. The proportional resonant controllers were applied, which is adaptive in nature in order to consider load dynamics.

Three injections with random angles were exploited to identify the optimum angle of the injected currents in [17], in which a general mathematical expression is presented that connects the voltage harmonic injection angle and current distortion. As the derived expression is a convex function, there exists a unique injection angle that minimizes overall current harmonic distortion.

The study presented in [18] showed that real Nonlinear loads in a weak MG with PVs do not necessarily lead to unacceptable harmonic levels. A proper share of PV panels can improve the voltage profile while keeping the grid in compliance with THD limits.

Voltage sag, the most common power quality issue in the power system when PVs are integrated, is investigated in [22], considering the stochastic nature of solar energy. Also, an innovative approach called a multi-objective control strategy to enhance the efficiency of grid-connected PVs, which specifically targets abnormal grid voltage situations, including distorted voltages, grid faults, and weak grids, is investigated.

The grid-connected inverters often employ a unit PCC voltage feedforward scheme as a common method to mitigate the impact of PCC voltage on the grid current. A feedforward scheme with excellent capability was suggested in [19] for rejecting harmonics, ensuring the injection of high-quality current.

PVs were exploited in [17] to neutralize the current harmonics using voltage harmonic injection angle. The optimum voltage injection angle was calculated by at least three injections with random angles. The salient point of the proposed method was that no need to know the type of grid connection, the converter harmonic properties, or the grid harmonic contents.

A technique based on fractional least mean square control with the power management strategy is presented in [20] for the PVs equipped with a battery system, which controls the converters to locally compensate load currents.

Reference generation is a key component of active filtering, which is a technique used to mitigate harmonics and other power quality issues in electrical systems. In an active filter, a control system is used to generate a reference signal that is used to control the operation of a power electronics device. The reference signal is generated based on measurements of the electrical parameters of the system, such as voltage and current. The reference signal is designed to cancel out the unwanted harmonics, thereby improving the quality of the power signal. Reference generation is a critical component of active filtering, as it determines the effectiveness of the filter in mitigating harmonics and other power quality issues. By generating a reference signal that cancels out unwanted harmonics, active filters can improve the quality of the power signal and ensure the reliable and safe operation of electrical systems [21], [22].

The Current Control Method (CCM) is another technique control method amongst virtual impedance control methods to regulate the output current. They are more robust to grid disturbances and variations in the virtual impedance parameters as CCM provides a more stable and predictable control mechanism for regulating the virtual impedance. They are simpler to design and implement, with reduced sensitivity to parameter variations: CCM-based VCMs exhibit lower sensitivity to changes in virtual impedance parameters compared to other VCMs. This is because the CCM provides a more stable and predictable control mechanism that is less affected by changes in the virtual impedance parameters [23], [24]. Exploiting CCM can lead to reduced harmonic distortion in the converter output, particularly in situations where there are multiple converters or other sensitive equipment connected to the same grid [10].

This paper is organized as follows. First, the concepts used in the proposed method are presented in more depth in section 2. The application of the Extremum Seeking Control (ESC) in the proposed methodology is investigated in part 3. The proposed method is described in section 4 and the details of modeling are presented in part 5. Then, section 6 discusses the results of implementing the suggested control strategy in the study case. Finally, the conclusion remarks are drawn in Section 7.

2. Concepts of the proposed method

The nonlinear loads create harmonic currents. One technique for mitigating each harmonic current is to inject another harmonic current with the same magnitude and opposite phase angle, which is known as harmonic current injection to decrease THD of PCC's voltage. This concept is depicted in Fig. 1. Note that i_i is the injected harmonic current, while i_L is the load harmonic current. Moreover, e_s and l_s are the voltage and the inductance of the source (the upstream network).

Fig. 2 shows the equivalent circuit model of h^{th} harmonic mitigation by injecting harmonic current. Note that I_{ih} and I_{Lh} are the phasors of the injected harmonic current and the load harmonic current, respectively. $\boldsymbol{V}_h$ is the phasor of PCC's harmonic voltage.

Decentralized RESs (especially PVs) can cancel grid voltages harmonic by injecting harmonic current with magnitude and phase angle equal to those of load harmonic current, $I_{ih} = I_{Lh}$, and $\theta_{ih} = \theta_{Lh}$. Thus, the nonlinear load current harmonic of the system is canceled out completely, which results in voltage harmonic cancelation. Usually, the available capacity of PV system limits the magnitude of I_ih. In such a case, the injected harmonic current magnitude must be set based on the available capacity of the PV system i.e., $I_{ih} < I_{Lh}$, but its phase is set equal to that of the load current harmonics $\theta_{ih} = \theta_{Lh}$. In this way, the voltage harmonic reduces to its minimum value.

3. Extremum Seeking Control (ESC)

The adaptive control methods are mostly developed for tracking a known reference trajectory or regulation to a known step value. ESC is a model-based control technique that seeks to optimize a performance index by adjusting a control parameter in real-time.

In applications with unknown parameters, ESC can perform quite well and keep an optimization function at the extremum. There are two main classes of ESC namely model-based and perturbation-based approaches [25].

The perturbation-based ESC is a kind of adaptive control algorithm that doesn't rely on a specific model of the system. It adjusts control parameters in real-time based on the system's unknown dynamics and the relationship between those parameters and the desired outcome.

The concept behind ESC involves:

a) introducing a sinusoidal signal to perturb a specific parameter value, and
b) observing how it affects the objective function (OF).

Through multiplication and integration of the OF signal with the same sinusoidal signal, the algorithm is able to estimate the gradient of the OF. Based on this estimation, the parameter value is updated in a way that moves it toward the optimal value that either maximizes or minimizes the OF. This process is repeated iteratively until the parameter value converges to the desired optimal value. Basically, ESC utilizes the relationship between the perturbed parameter and the OF to iteratively improve the parameter value and ultimately optimize the outcome.

The proposed block diagram of the ESC via perturbation method, which is inspired from [26] is depicted in Fig. 3.

A_h controls the magnitude of the perturbation and ω_h controls the speed of the perturbation.

The ESC method used in this study does not rely on a traditional system model (e.g., state-space or transfer function). Instead, it operates as a perturbation-based technique. The ‘model’ in this context is implicitly formed by the system's response to the perturbation, which provides information about the gradient of the performance index, the THD at the PCC in this case. The controller adjusts the harmonic current injection in real-time based on this estimated gradient, ensuring harmonic mitigation. As the load and grid impedances are unknown, the method is designed to operate without requiring prior knowledge of these parameters, making it well-suited for dynamic microgrid environments. Therefore, the ESC is the perturbation-based scheme in which the estimated gradient (as an excitation signal) is added to the input, in order to extract the information. From Fig. 3, it can be concluded that:

$$y = f(x, \alpha(x, \theta)) \tag{1}$$

Where the perturbation signal is;

$$\theta = \hat{\theta} + A_h \sin(\omega_h t) \tag{2}$$

This formula is used to perturb the system's parameter θ in order to find its optimal value. A_h is the amplitude of the perturbation signal and ω_h is the frequency of the perturbation signal. These parameters are critical for the performance of ESC, and their tuning depends on the specific system and control objectives.

A proof of stability of an ESC by employing averaging and singular perturbation analysis was presented in [26]. The parameters in ESC can be tuned through various methods. A few common approaches are manual tuning, trial-and-error, optimization algorithms, and system identification.

4. Proposed Method

It is assumed that phasor parameters (magnitude and phase) of the load harmonic current have uncertainty. Furthermore, the load impedances and the Thevenin equivalent impedance of the network are unknown.

The concept of the proposed method is represented by a phasor diagram in Fig. 4. This diagram helps visualize the harmonic currents and their effects on the system. As shown in the diagram, the presence of specific current harmonics (I_{Lh}) can be identified by its voltage harmonic ($\boldsymbol{V}_h$). In addition, $\boldsymbol{Z}_h$ represents the circuit impedance at h^{th} harmonic.

The PCC voltage waveform in the time domain is:

$$v(t) = v_{PCC}(t) = \sum_{k\in\mathbb{N}} v_{2k-1}(t) \tag{3}$$

Using phasor $\boldsymbol{V}_h \triangleq V_h \measuredangle \theta_h$ for each voltage harmonic, the voltage PCC amplitude can be expressed as:

$$V_{PCC}^2 = \sum_{h=2k-1,k\in\mathbb{N}} V_h^2 \tag{4}$$

Where:

$$\boldsymbol{V}_h = \boldsymbol{Z}_h(\boldsymbol{I}_{ih} - \boldsymbol{I}_{Lh}) \tag{5}$$

$$\boldsymbol{I}_{ih} \triangleq I_{ih} \measuredangle \theta_{ih} \tag{6}$$

$$\boldsymbol{I}_{Lh} \triangleq I_{Lh} \measuredangle \theta_{Lh} \tag{7}$$

$$\boldsymbol{Z}_h \triangleq Z_h \measuredangle \theta_{zh} \tag{8}$$

$$V_h^2 = Z_h^2 |\boldsymbol{I}_{ih} - \boldsymbol{I}_{Lh}|^2 \tag{9}$$

$$V_h^2 = Z_h^2 \{I_{ih}^2 + I_{Lh}^2 - 2I_{ih}I_{Lh}\cos(\theta_{ih} - \theta_{Lh}) \tag{10}$$

According to (9), to cancel or mitigate a voltage harmonic (V_h), the magnitude of the injected harmonic current (I_{ih}) must be equal to or smaller than the load harmonic current magnitude (I_{Lh}). In other words:

$$I_{ih} \leq I_{Lh} \tag{11}$$

Moreover, the current capacity of the PV inverter must not be violated. According to (10), to have maximum voltage harmonic mitigation, the phase angle of the injected harmonic current (θ_{ih}) must be equal to that of the load harmonic current (θ_{Lh}).

To implement ESC for grid voltage-harmonics mitigation, the control system adjusts θ_{ih} and I_{ih} to minimize voltage RMS value, using a feedback loop to continuously monitor and control the system in real time.

The parameters of the ESC strategy are tuned using the NSGA-II, a heuristic optimization method. This approach was employed to optimize the control parameters for harmonic mitigation, balancing performance and computational efficiency. While the primary focus of this work is on the ESC method itself, NSGA-II was used to fine-tune the controller settings to achieve optimal harmonic reduction at the Point of Common Coupling (PCC).

5. Modeling Details

5.1. PV and Grid

Available solar power is assumed to be a constant value. The single-line diagram of the test case is illustrated in Fig. 5. The specifications of the upstream grid are presented in Table 2.

5.2. Extremum Seeking Control (ESC)

Adjusting key parameters of the ESC control algorithm assures optimal system operation. In the proposed method, the general steps to adjust the control parameters are:

- The OF is to minimize the RMS voltage of PCC (V_{PCC}):
- The angle of the injected harmonic current is used as a perturbation signal to estimate the gradient of the OF. Note that the perturbation signal must be suitable for the dynamics of the system and should not cause undue stress or oscillation in the system.
- The minimization is ended when a minimum RMS voltage V_{PCC}, (OF) is reached.

In order to implement the ESC algorithm in the system, the control parameters must be adjusted such as gains of the feedback loops or appropriate filter parameters to reduce the noise.

In this paper, a voltage source inverter is controlled by a current controller which behaves as an injecting current source into the grid.

The harmonic spectrum is defined by the amplitudes for each harmonic order and angle. For the harmonic spectrum in the example, all three phases will inject the same harmonic current magnitude. However, the appropriate angles are obtained via the ESC algorithm.

Note that when $\boldsymbol{V_{PCC}}$ is chosen as the objective function, its minimization automatically reduces the harmonic components. This means that ESC indirectly optimizes the harmonic profile by minimizing the differential of the harmonic content instead of explicitly computing harmonic distortion. Therefore, according to Fig. 4, Eq. (9) and (10), the PCC harmonic as the OF is:

$$J = \Delta V_h^2 = Z_h^2 \Delta |\boldsymbol{I}_{ih} - \boldsymbol{I}_{Lh}|^2 \tag{12}$$

$$|\boldsymbol{I}_{ih} - \boldsymbol{I}_{Lh}|^2 = I_{ih}^2 + I_{Lh}^2 - 2 I_{Lh} I_{ih} \cos(\theta_{Lh} - \theta_{ih}) \tag{13}$$

Assuming I_{ih} and I_{Lh} are constant during adjustments, concludes $\Delta I_{ih}, \Delta I_{Lh} = 0$. Therefore, Eq. (13) concludes:

$$J = \Delta |\boldsymbol{I}_{ih} - \boldsymbol{I}_{Lh}|^2 = 2 I_{ih0} I_{Lh0} \sin(\theta_{Lh} - \theta_{ih}) \Delta\theta_{ih} \tag{14}$$

As shown in Fig. 6, by multiplying and integrating the OF signal with the same sinusoidal signal, the algorithm estimates the gradient of the OF. This gradient provides information about the direction and magnitude of change needed to optimize the OF. If we assume that $\Delta\theta_{ih} = A_h \sin(\omega_h t)$ and is introduced as the perturbation source, then:

$$J = \Delta |\boldsymbol{I}_{ih} - \boldsymbol{I}_{Lh}|^2 = 2 I_{ih0} I_{Lh0} \sin(\theta_{Lh} - \theta_{ih}) A_h \sin(\omega_h t) \tag{15}$$

6. Simulation Results and Discussion

6.1. ESC Implementation

The ESC module designed for minimizing harmonic distortion as depicted in Fig. 6. The same structural approach is consistently applied to mitigate all other harmonic components. Furthermore, the parameters of the proposed technique for different harmonic orders are systematically presented in Table 3, ensuring a comprehensive understanding of the control strategy and its adaptability to various harmonic frequencies.

6.2. Outputs of the Controllers

The nonlinear current generated by the load, which forms the primary focus of our mitigation efforts, is detailed in Table 4. This table presents a comprehensive breakdown of the harmonic distortion caused by the load, highlighting the specific harmonic orders and their corresponding amplitudes. These nonlinear currents represent a significant challenge for the system, as they can lead to inefficiencies, overheating of equipment, and potential voltage distortion. To better understand the context of this issue, it is useful to first examine the signals produced by the ESC controllers, as illustrated in Fig. 7.

A close inspection of these figures reveals the dynamic response of the ESC controllers under the influence of these nonlinear loads. The controllers' performance, including their ability to stabilize the system and mitigate the effects of harmonic distortion, can be observed in these figures. This sets the stage for evaluating how effectively the ESC controllers are addressing the disturbances and improving the overall power quality within the system. The x-axis represents time in seconds, while the y-axis represents angles in degrees. The blue line represents θ_3 and the green line represents θ_7 which have positive values and follow an increasing pattern. The other colors orange, red, and lavender denote θ_5, θ_{11}, and θ_{13}, respectively, and have negative values and follow a decreasing pattern. As can be seen, there is no sudden spike in the growth rate of the curves and they settle at the worst case at around 3.5 seconds. This suggests that ESC presents good capability in a reasonable time scale in providing suitable values for the angles required to diminish the harmonics.

6.3. Results and Discussion

The proposed ESC method has a moderate budget because it uses existing inverter capacity without requiring extensive additional hardware or sensors. Therefore, it is cost-effective compared to advanced techniques like APFs, MPC, or AI-based approaches.

Given the financial comparability between the proposed ESC method and passive filtering, a direct comparison is both relevant and insightful. Passive filters, while cost-effective and easy to implement, provide a fixed solution that may not be as adaptable to varying load conditions. In contrast, ESC offers real-time optimization, allowing it to better handle dynamic changes and unknown system parameters. Although passive filters can effectively mitigate harmonics under steady-state conditions, the ESC method provides superior harmonic reduction, particularly in scenarios where load and grid impedances are uncertain. Moreover, passive filters are generally more effective at reducing low-order harmonics (e.g., 3rd, 5th, 7th), but may be less effective at mitigating higher-order harmonics or those with non-sinusoidal characteristics.

This comparison highlights the potential of ESC as a flexible, performance-driven solution that remains cost-competitive with traditional passive filtering methods, particularly in complex MG environments where dynamic conditions prevail.

In this study, the proposed method is compared with APF, particularly with the approach outlined in reference [27], which highlights a significant reduction in the required rating of the active filter compared to conventional APFs. This feature discussed as a strength of the APF method in [27], demonstrates that a smaller filter can achieve similar harmonic mitigation performance. In contrast, the ESC method, while not relying on the reduction of filter rating, offers dynamic and real-time optimization for harmonic mitigation, which makes it particularly advantageous in systems with unknown or fluctuating load conditions.

The APF must handle approximately 17.82 (A) RMS of harmonic current according to Table 4. For control of the inverter, the SRF method is used to extract the harmonic components (above the 3rd harmonic) which requires high-speed current sensors and a digital controller capable of performing real-time FFT analysis to identify the harmonic content. The controller tracks the harmonic components (5th, 7th, 11th, 13th) and commands the inverter to inject currents with appropriate magnitudes and phase shifts to cancel these harmonic currents. A PWM technique with a switching frequency of 10 kHz is used to ensure smooth operation. Table 5 provides a comprehensive summary of the key characteristics of the APF system. These parameters are crucial for understanding the operational performance and design specifications of the APF, which plays a vital role in mitigating harmonic distortion.

THD is used as a critical criterion for comparing the performance of the ESC and APF. Expressed as a percentage, THD is calculated by dividing the RMS value of the harmonic components by the RMS value of the fundamental frequency. This allows for an objective assessment of how each system reduces harmonic distortion, with lower THD values indicating more effective mitigation and better overall power quality. The lower the THD value, the less distortion exists in the signal.

Table 6 presents a comparative analysis of THD levels for both voltage (THD_v (%)) and current (THD_i) within the system under different mitigation scenarios. The table highlights the effectiveness of two mitigation techniques, the ESC and the APF, in reducing harmonic distortion compared to the baseline scenario of "Without Mitigation." The results clearly demonstrate a significant reduction in both voltage and current THD when either the ESC or the APF is implemented. In the absence of any mitigation, the system exhibits a voltage THD of 3.70% and a considerably higher current THD of 30.15%. This indicates a substantial level of harmonic distortion present within the system.

Upon the introduction of the ESC, the voltage THD is drastically reduced to 0.29% and the current THD to 2.40%. This represents a remarkable improvement, suggesting the ESC's high effectiveness in mitigating harmonic distortion. Similarly, the APF also contributes to a reduction in harmonic distortion, achieving a voltage THD of 0.69% and a current THD of 5.61%. While the APF's performance is not as pronounced as the ESC's, it still offers a significant improvement compared to the "Without Mitigation" scenario.

Both the ESC and the APF demonstrate their capabilities in reducing THD levels, with the ESC exhibiting a superior performance in this specific application. This data underscores the importance of harmonic mitigation for maintaining power quality and ensuring the efficient operation of electrical systems.

Fig. 8 presents a comparative analysis of the voltage waveforms at the Point of Common Coupling (PCC) for phase A under various mitigation scenarios, spanning a 20 (ms) period. The figure illustrates the effectiveness of both the proposed ESC and a conventional APF in reducing harmonic distortion. The baseline waveform, representing the load current ("Without Mitigation" case), is depicted by a dotted red line. The solid blue line represents the waveform when the APF is active, while the dashed green line corresponds to the ESC-based mitigation. Visual inspection of Fig. 8 reveals distinct differences in the waveform characteristics between the mitigation techniques and the unmitigated case, suggesting varying degrees of harmonic reduction. However, a more quantitative assessment of harmonic content is necessary to draw definitive conclusions about the performance of each method. Therefore, Fig. 9 provides a comparative spectral analysis using FFT bar charts. This figure presents the harmonic magnitudes for the APF (blue bars with vertical hatches) and the ESC (green bars with horizontal hatches).

The analysis reveals that the ESC demonstrates superior performance in mitigating lower-order harmonics, specifically up to the 7^{th} harmonic. Conversely, the APF exhibits better performance in attenuating higher-order harmonics, notably the 11^{th} and 13^{th}. This observation highlights the distinct frequency-domain characteristics of each mitigation technique and suggests that their effectiveness may vary depending on the specific harmonic profile of the system. However, considering that lower-order harmonics typically possess larger amplitudes and therefore contribute more significantly to the overall THD, the ESC's superior performance in this range results in a lower overall THD, as demonstrated in Table 6. This observation highlights the distinct frequency-domain characteristics of each mitigation technique and suggests that their effectiveness may vary depending on the specific harmonic profile of the system, but in this specific case, the ESC offers better overall performance.

Fig. 10 provides a comparative view of the PCC voltage waveforms for phase A under different harmonic mitigation strategies, covering a 20 (ms) interval. The plot showcases the performance of the proposed ESC against the APF in mitigating harmonic distortion. A dotted red line marks the baseline, representing the unmitigated scenario. The APF's performance is shown by a solid blue line, while the ESC's effect is illustrated by a dashed green line. A visual inspection of Fig. 10 reveals a reduction in the waveform suggesting varying degrees of harmonic suppression. However, a more rigorous analysis of the harmonic content is required to make definitive judgments about the efficacy of each method. Therefore, Fig. 11 presents a comparative frequency-domain analysis using FFT bar graphs. This figure compares the voltage harmonic amplitudes produced by the APF (blue bars with vertical hatching) and the ESC (green bars with horizontal hatching). The analysis indicates that the ESC excels at mitigating lower-order harmonics, particularly those up to the 7th. Conversely, the APF demonstrates superior attenuation of higher-order harmonics, especially the 11th and 13th. Nevertheless, because lower-order harmonics typically have larger magnitudes and thus a greater impact on the overall THD, the ESC's improved performance in this lower frequency range leads to a lower overall THD, as confirmed by the data in Table 6.

6.4. Challenges

The simulations conducted in this section showcased the feasibility and effectiveness of incorporating PV systems with converters to enable sustainable operation and mitigate harmonic contents. It is worth noting that the proposed method might have some impacts on the capacitor lifetime in the PV inverter mitigating some harmonics.

An investigation in [27] showed that the 5th harmonic mitigation in the grid voltage might have a possible DC-link capacitor lifetime reduction of up to 52% which is the direct consequence of the oscillations in voltage and current of the dc-link. Accordingly, this lifetime reduction could be an awareness for designers during the design process and can be an interesting issue for further research in order to prevent unforeseen early breakdown of the inverters caused by DC-link failures.

A shift in the approach to harmonic control, transitioning from local compensation to system-level mitigation is discussed in [28]. However, current system-level harmonic mitigation methods necessitate rapid data exchange for real-time phase synchronization among multiple buses, which compromises the practicality of these methods.

ESC can be a complex and computationally intensive technique, as it requires real-time optimization of a performance metric using a feedback loop. Additionally, ESC requires accurate modeling of the system and careful tuning of the control parameters to ensure that it operates effectively.

7. Conclusion

This paper investigates the role of PV inverters, connected to distribution grids, in mitigating harmonic content in PCC voltage. Utilizing PV systems offers a promising solution for integrating renewable energy sources into grids and microgrids. However, the proliferation of nonlinear loads generates current harmonics that can degrade power quality. Solar power systems can address these power quality challenges by leveraging PV inverters for PCC voltage harmonic mitigation. The key advantage of Extremum Seeking Control (ESC) for this purpose lies in its adaptability to system changes and real-time optimization. This is particularly beneficial in applications where load or electrical system characteristics vary over time.

This paper exploits ESC to enhance the performance of PV inverters in mitigating PCC voltage harmonics. Critically, the presented method requires no prior knowledge of grid's current harmonic content. Simulations demonstrate that the proposed control strategy effectively reduces voltage THD well below the IEEE Std. 519-2014 limit of 8% for low-voltage grids. Specifically, the simulations showed a reduction of THD_v from 3.70% without mitigation to 0.29% with the proposed ESC, representing a 92% improvement.

Furthermore, comparisons with an APF demonstrated the superior performance of the ESC, which achieved a THD_v of 0.29% compared to the APF's 0.69% (an 81% reduction from the unmitigated case).

APF was chosen as the benchmark for comparison because it is one of the most widely used solutions for harmonic mitigation in microgrids due to its functionality, adaptability, and well-established control strategies. Additionally, a balanced trade-off between performance, complexity, and budget is offered by APFs, making them a practical choice for real-world applications. By comparing the proposed ESC-based method with APF, a fair and meaningful assessment of its advantages in improving power quality is provided. These results validate the efficacy of the proposed approach, establishing the ESC method as a practical, cost-effective, and adaptable solution for improving power quality in PV-based grids or microgrid systems.

8. References

[1] "30% by 2030: A New Target for the Solar+ Decade," 2021.

[2] P. Verma, R. Garg, and P. Mahajan, "ASYMMETRICAL FUZZY LOGIC CONTROL BASED MPPT ALGORITHM FOR STAND-ALONE PV SYSTEM UNDER PARTIALLY SHADED CONDITIONS," *Scientia Iranica*, vol. 0, no. 0, pp. 0–0, Feb. 2019, doi:2010.24200/sci.2019.51737.2338.

[3] H. Karimi, M. Simab, and M. Nafar, "Enhancement of Power Quality Utilizing Photovoltaic fed D-STATCOM Based on Zig-Zag Transformer and Fuzzy Controller," *Scientia Iranica*, vol. 0, no. 0, pp. 0–0, Oct. 2020, doi: 10.24200/sci.2020.54952.3998.

[4] Y. W. Li and J. He, "Distribution System Harmonic Compensation Methods: An Overview of DG-Interfacing Inverters," *IEEE Industrial Electronics Magazine*, vol. 8, no. 4, pp. 18–31, Dec. 2014, doi: 10.1109/MIE.2013.2295421.

[5] M. Prasad, A. K. Akella, and A. Youssef, "Design and Analysis of Solar Photovoltaic fed Z-Source Inverter based Dynamic Voltage Restorer," *Scientia Iranica*, vol. 0, no. 0, pp. 0–0, Feb. 2019, doi: 10.24200/sci.2019.51096.2000.

[6] M. Bajaj and A. K. Singh, "Grid integrated renewable DG systems: A review of power quality challenges and state-of-the-art mitigation techniques," *Int J Energy Res*, vol. 44, no. 1, pp. 26–69, Jan. 2020, doi: 10.1002/er.4847.

[7] B. Adineh, R. Keypour, P. Davari, and F. Blaabjerg, "Review of Harmonic Mitigation Methods in Microgrid: From a Hierarchical Control Perspective," *IEEE J Emerg Sel Top Power Electron*, vol. 9, no. 3, pp. 3044–3060, Jun. 2021, doi: 10.1109/JESTPE.2020.3001971.

[8] X. Liang and C. Andalib -Bin- Karim, "Harmonics and Mitigation Techniques Through Advanced Control in Grid-Connected Renewable Energy Sources: A Review," *IEEE Trans Ind Appl*, vol. 54, no. 4, pp. 3100–3111, Jul. 2018, doi: 10.1109/TIA.2018.2823680.

[9] M. L. Duc, L. Hlavaty, P. Bilik, and R. Martinek, "Harmonic Mitigation Using Meta-Heuristic Optimization for Shunt Adaptive Power Filters: A Review," *Energies (Basel)*, vol. 16, no. 10, p. 3998, May 2023, doi: 10.3390/en16103998.

[10] I. Khan, A. S. Vijay, and S. Doolla, "Nonlinear Load Harmonic Mitigation Strategies in Microgrids: State of the Art," *IEEE Syst J*, vol. 16, no. 3, pp. 4243–4255, Sep. 2022, doi: 10.1109/JSYST.2021.3130612.

[11] R. Musona and I. Serban, "Differential Single-Phase Inverters With Active Power Decoupling: A Survey," *IEEE Access*, vol. 11, pp. 53654–53670, 2023, doi: 10.1109/ACCESS.2023.3280228.

[12] V. Boscaino *et al.*, “Grid-connected photovoltaic inverters: Grid codes, topologies and control techniques,” *Renewable and Sustainable Energy Reviews*, vol. 189, p. 113903, Jan. 2024, doi: 10.1016/j.rser.2023.113903.

[13] M. S. Nkambule, A. Nabil Hasan, and T. Shongwe, “Advanced Control Strategies for Photovoltaic Power Quality and Maximum Power Point Tracking Optimization,” *IEEE Access*, vol. 12, pp. 74456–74481, 2024, doi: 10.1109/ACCESS.2024.3404497.

[14] A. Taghvaie, T. Warnakulasuriya, D. Kumar, F. Zare, R. Sharma, and D. M. Vilathgamuwa, “A Comprehensive Review of Harmonic Issues and Estimation Techniques in Power System Networks Based on Traditional and Artificial Intelligence/Machine Learning,” *IEEE Access*, vol. 11, pp. 31417–31442, 2023, doi: 10.1109/ACCESS.2023.3260768.

[15] Y. Naderi, S. H. Hosseini, S. Ghassem Zadeh, B. Mohammadi-Ivatloo, J. C. Vasquez, and J. M. Guerrero, “An overview of power quality enhancement techniques applied to distributed generation in electrical distribution networks,” *Renewable and Sustainable Energy Reviews*, vol. 93, pp. 201–214, Oct. 2018, doi: 10.1016/j.rser.2018.05.013.

[16] P. S. Prasad and A. M. Parimi, “Harmonic Mitigation in Grid Connected and Islanded Microgrid Via Adaptive Virtual Impedance,” in *2020 IEEE International Conference on Power Electronics, Smart Grid and Renewable Energy (PESGRE2020)*, IEEE, Jan. 2020, pp. 1–6. doi: 10.1109/PESGRE45664.2020.9070598.

[17] I. D. Bouloumpasis, P. N. Vovos, and K. G. Georgakas, “Voltage harmonic injection angle optimisation for grid current harmonics using a PV converter,” *IET Power Electronics*, vol. 12, no. 9, pp. 2382–2388, Aug. 2019, doi: 10.1049/iet-pel.2018.5608.

[18] S. M. Ahsan, H. A. Khan, A. Hussain, S. Tariq, and N. A. Zaffar, “Harmonic Analysis of Grid-Connected Solar PV Systems with Nonlinear Household Loads in Low-Voltage Distribution Networks,” *Sustainability*, vol. 13, no. 7, p. 3709, Mar. 2021, doi: 10.3390/su13073709.

[19] Cheng Wang; Xuehua Wang; Yuying He; Xinbo Ruan, “A Passivity-Based Weighted Proportional-Derivative Feedforward Scheme for Grid-Connected Inverters With Enhanced Harmonic Rejection Ability,” *IEEE J Emerg Sel Top Power Electron*, vol. 11, no. 4, pp. 3656–3668, 2023, doi: https://doi.org/10.1109/JESTPE.2021.3121410.

[20] G. Modi and B. Singh, “F-LMS Adaptive Filter Based Control Algorithm With Power Management Strategy for Grid Integrated Rooftop SPV-BES System,” *IEEE Trans Sustain Energy*, vol. 14, no. 2, pp. 987–999, Apr. 2023, doi: 10.1109/TSTE.2022.3231684.

[21] R. Kumar, “Fuzzy particle swarm optimization control algorithm implementation in photovoltaic integrated shunt active power filter for power quality improvement using hardware-in-the-loop,” *Sustainable Energy Technologies and Assessments*, vol. 50, p. 101820, Mar. 2022, doi: 10.1016/j.seta.2021.101820.

[22] N. M. Dehkordi, N. Sadati, and M. Hamzeh, “A Robust Backstepping High-Order Sliding Mode Control Strategy for Grid-Connected DG Units With Harmonic/Interharmonic Current Compensation Capability,” *IEEE Trans Sustain Energy*, vol. 8, no. 2, pp. 561–572, Apr. 2017, doi: 10.1109/TSTE.2016.2611383.

[23] C. Blanco, D. Reigosa, J. C. Vasquez, J. M. Guerrero, and F. Briz, “Virtual Admittance Loop for Voltage Harmonic Compensation in Microgrids,” *IEEE Trans Ind Appl*, vol. 52, no. 4, pp. 3348–3356, Jul. 2016, doi: 10.1109/TIA.2016.2547362.

[24] M. A. Aboushal and M. M. Z. Moustafa, “A new unified control strategy for inverter-based micro-grid using hybrid droop scheme,” *Alexandria Engineering Journal*, vol. 58, no. 4, pp. 1229–1245, Dec. 2019, doi: 10.1016/j.aej.2019.10.006.

[25] D. Dochain, M. Perrier, and M. Guay, “Extremum seeking control and its application to process and reaction systems: A survey,” *Math Comput Simul*, vol. 82, no. 3, pp. 369–380, Nov. 2011, doi: 10.1016/j.matcom.2010.10.022.

[26] M. Krstić and H.-H. Wang, “Stability of extremum seeking feedback for general nonlinear dynamic systems,” *Automatica*, vol. 36, no. 4, pp. 595–601, Apr. 2000, doi:2010.1016/S0005-1098(99)00183-1.

[27] H. Fujita and H. Akagi, “A practical approach to harmonic compensation in power systems-series connection of passive and active filters,” *IEEE Trans Ind Appl*, vol. 27, no. 6, pp. 1020–1025, 1991, doi: 10.1109/28.108451.

[28] Z. Yang *et al.*, “A System-Level Harmonic Control Method Based on Multibus Voltage Detected APF Without Exact Phase Synchronization,” *IEEE J Emerg Sel Top Power Electron*, vol. 11, no. 3, pp. 2618–2631, Jun. 2023, doi: 10.1109/JESTPE.2023.3267021.

list of captions

Fig. 1. Equivalent circuit for grid with nonlinear load and PV for injecting required harmonic current.

Fig. 2. Equivalent circuit for harmonic mitigation by injecting harmonic current in phase with load harmonic current.

Fig. 3. ESC using the perturbation method inspired from [26].

Fig. 4. The phasor diagram for the proposed voltage harmonic mitigation by injecting an opposite current.

Fig. 5. The single-line diagram of the first test case (as modeled in PSCAD).

Fig. 6. The ESC module implementation

Fig. 7. Different angles produced by the ESC.

Fig. 8. The waveform plot (phase A) of different angles produced by the ESC and the APF

Fig. 9. FFT comparison of the THD_i and for the ESC and the APF.

Fig. 10. Comparison of the voltage waveforms for the ESC and the APF

Fig. 11. Comparison of voltage harmonics (THD_v) in the ESC and the APF

Table 1- Summary of Key Issues and Techniques Addressed in Selected References

Table 2- The parameters of the grid

Table 3- The parameters of the control system

Table 4- Comparisons of THDs in the system

Table 5- Summary of APF characteristics

Table 6- Comparisons of THDs in the system

Table 1- Summary of Key Issues and Techniques Addressed in Selected References

Ref.	[6]	[7]	[8]	[9]	[10]	[11]	[12]	[13]	[14]	[15]
Voltage and Frequency Fluctuations	×	×	×	×				×	×	
Harmonics Distortion	×	×	×	×	×			×	×	×
FRT Capability	×									
Reactive Power Support	×							×		
Mitigation Techniques	×	×	×	×	×		×	×	×	×
Control Algorithm		×	×	×	×	×	×	×		×
Machine Learning									×	
Harmonic Propagation and Interaction		×	×	×	×			×		
Harmonic Detection			×		×			×		×
Optimization Methods		×		×						×

Table 2- The parameters of the grid

Parameter	r_g	L_g	V_s
Unit	ohm	mH	V
Value	0.3	3	200

Table 3- The parameters of the control system

Harmonic Order (h)	ω_h	A_h	B_h	K_h
3	30	-0.016	-0.001	30
5	70	0.0095	0.001	337
7	180	-0.011	0.001	125
11	190	0.045	0.005	323
13	230	0.007	0.0005	22

Table 4- Comparisons of THDs in the system

Harmonic Order	Amplitude	Phase angle (a)
	A	degree
3	16.5	9
5	9.9	-125
7	7.0	46
11	4.5	-164
13	3.8	-5

Table 5- Summary of APF characteristics

Parameter	Unit	Value
Rated apparent power	kVA	21.3
Switching frequency	kHz	10
Dc link voltage	V	1225
DC capacitor	μF	440
Inductance	mH	14

Table 6- Comparisons of THDs in the system

Scenario	THD_v (%)	THD_i (%)
Without Mitigation	3.70	30.15
ESC	0.29	2.40
APF	0.69	5.61

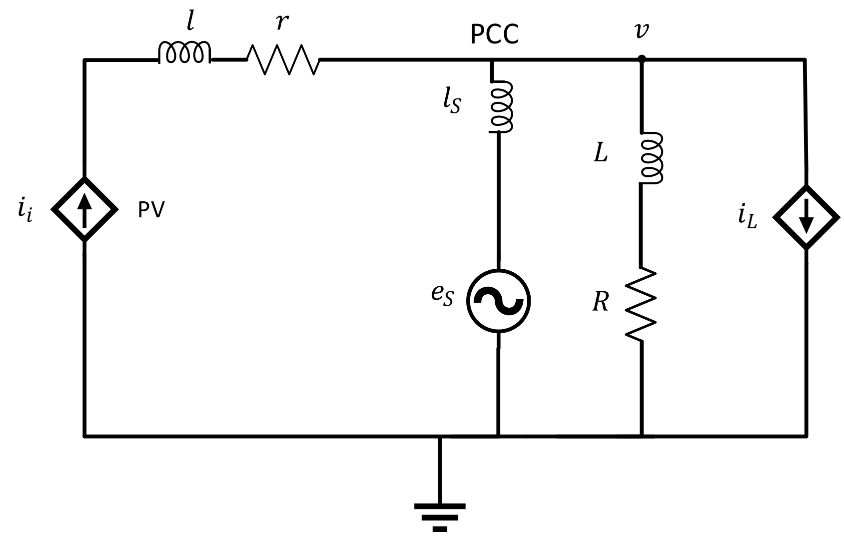

Fig. 1. Equivalent circuit for grid with nonlinear load and PV for injecting required harmonic current.

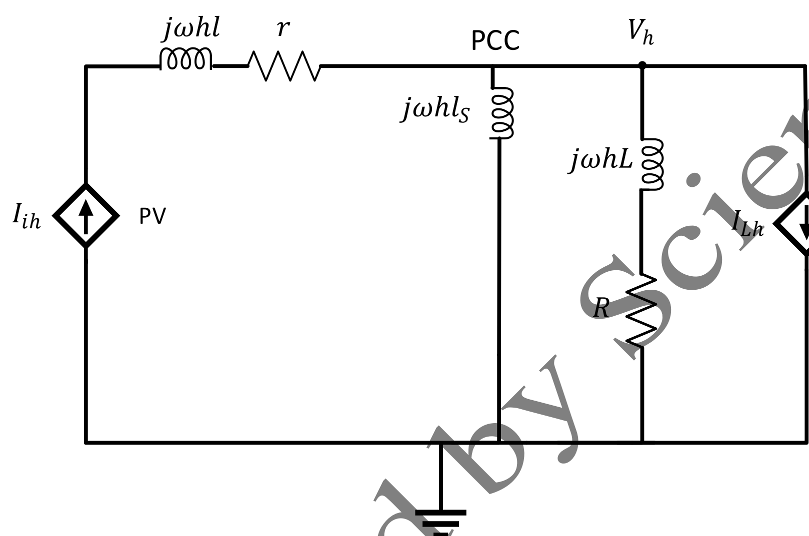

Fig. 2. Equivalent circuit for harmonic mitigation by injecting harmonic current in phase with load harmonic current.

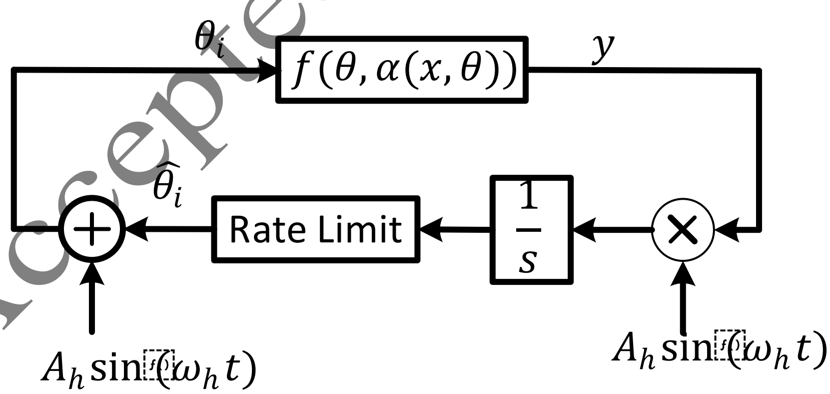

Fig. 3. ESC using the perturbation method inspired from [26].

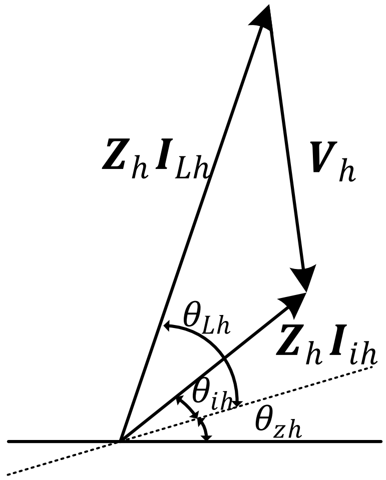

Fig. 4. The phasor diagram for the proposed voltage harmonic mitigation by injecting an opposite current.

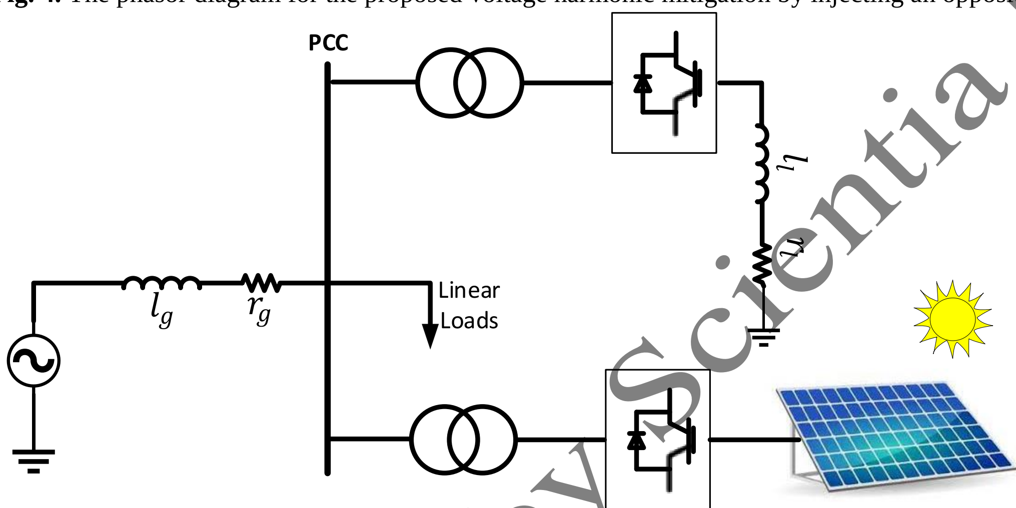

Fig. 5. The single-line diagram of the first test case (as modeled in PSCAD).

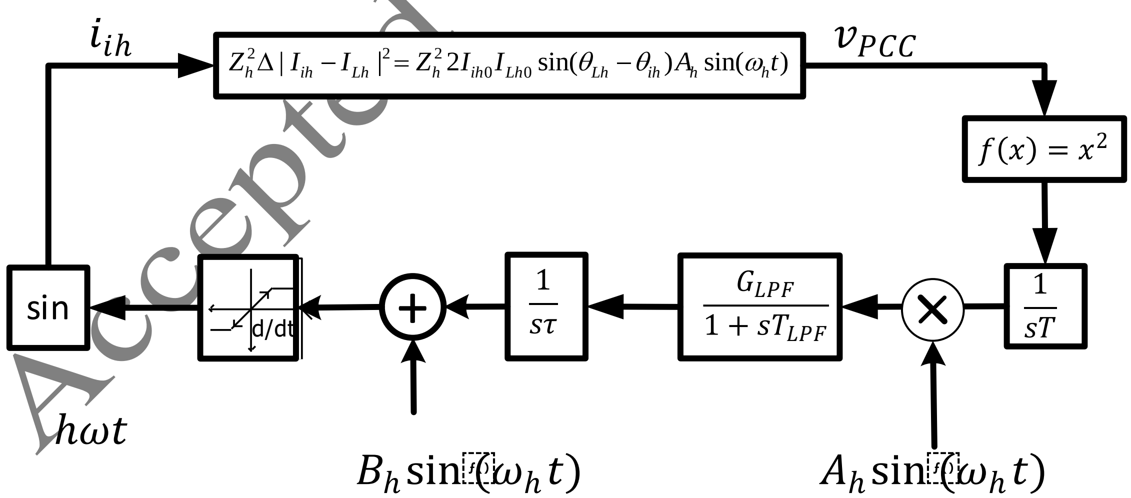

Fig. 6. The ESC module implementation

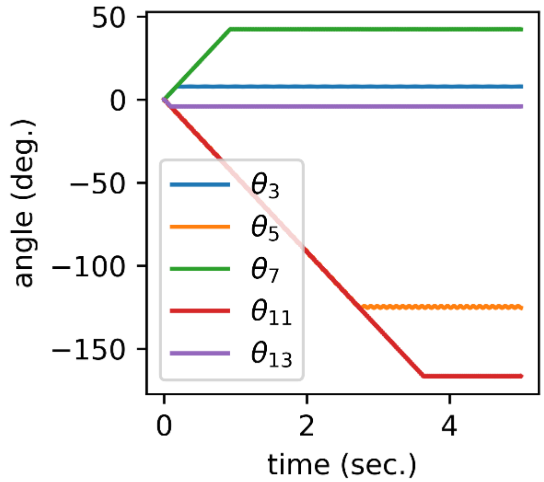

Fig. 7. Different angles produced by the ESC.

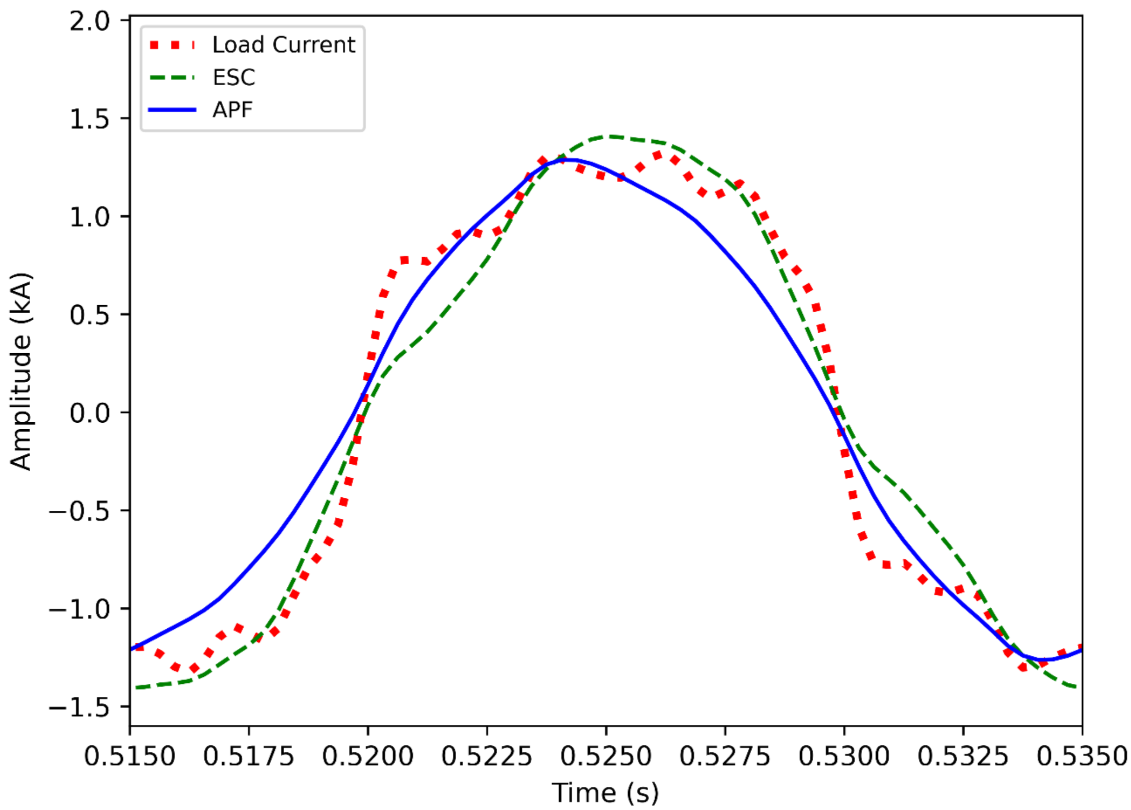

Fig. 8. The waveform plot (phase A) of different angles produced by the ESC and the APF

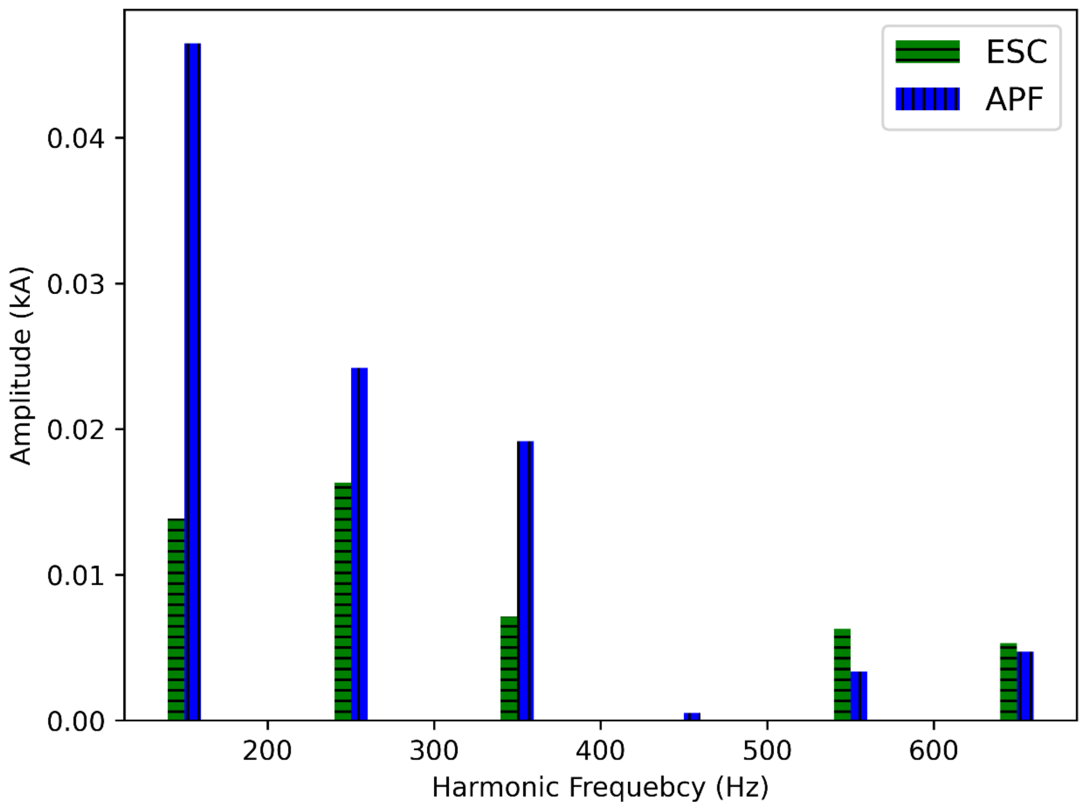

Fig. 9. FFT comparison of the THD_i and for the ESC and the APF.

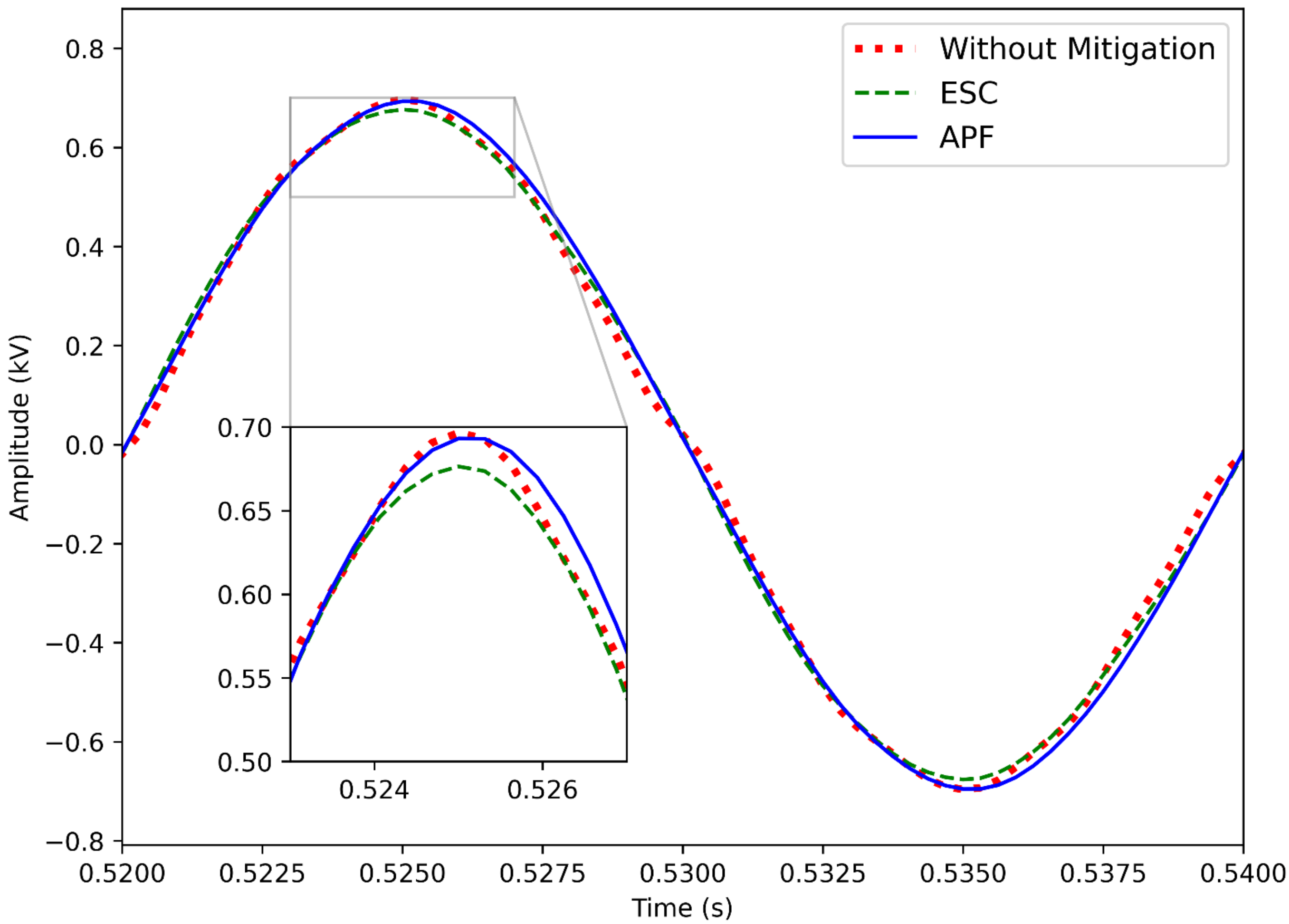

1
2 **Fig. 10.** Comparison of the voltage waveforms for the ESC and the APF

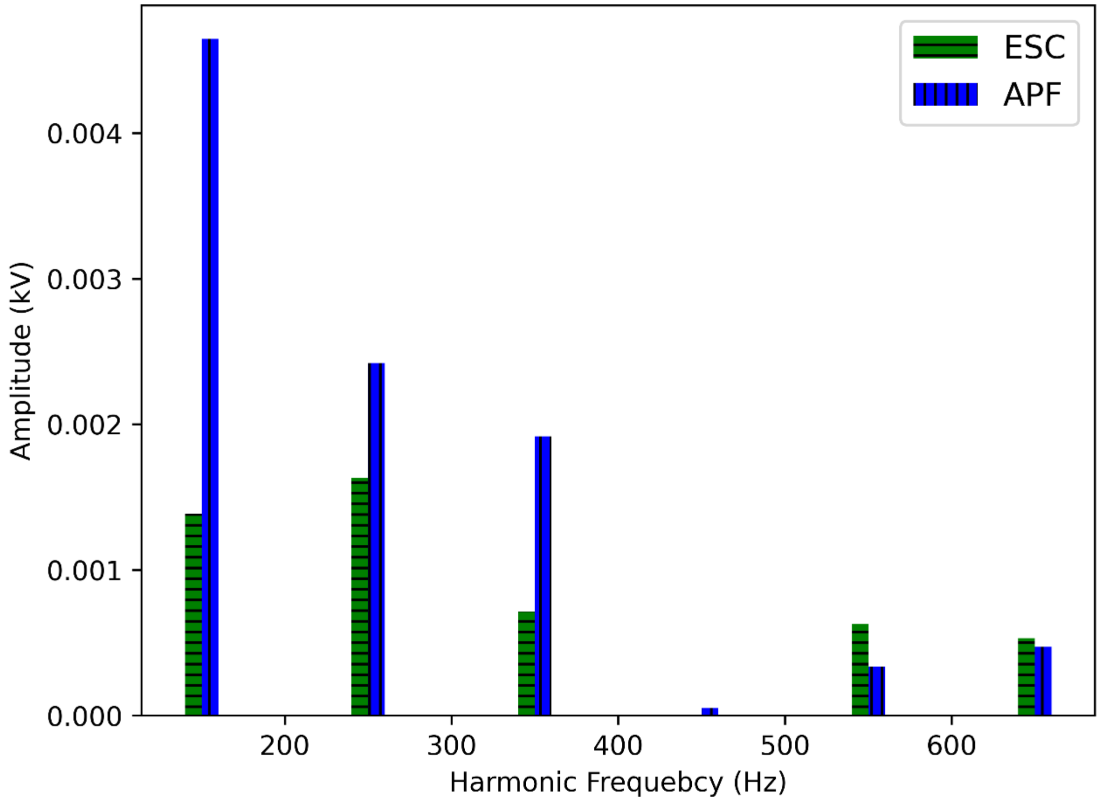

١
٢ **Fig. 11.** Comparison of voltage harmonics (THD_v) in the ESC and the APF
٣
٤

Biographies:

S. Masoud Tabatabaei Jebeli received the B.S. and M.S degrees in electrical engineering from Kashan University and Isfahan University of Technology, Iran, in 2011 and 2014 respectively. He is currently pursuing toward Ph.D. in electrical engineering department of Isfahan University, Iran, with a concentration on power systems.

Seyed M. Madani (SM'17) received the Ph.D. degree from the Eindhoven University of Technology, Eindhoven, the Netherlands, in 1999, in electrical power engineering. He is currently an Associate Professor of electrical power engineering at the University of Isfahan, Isfahan, Iran. His research interests include renewable energy.

M. Mojiri received the Ph.D. degree in electrical engineering from the IUT, Isfahan, Iran, in 2005. Since 2009, he has been a Faculty Member with the Department of Electrical and Computer Engineering, Isfahan University of Technology. His current research interests include adaptive control as applied to power systems.

Ebrahim Karimi received his Ph.D. degree from the Isfahan University of Technology, Isfahan, Iran, in 2015, in electrical power engineering. He is currently the director of Persian Danesh Isfahan. His research interests include decarbonization and uncertainty modeling in power systems